

# Optimal sensor location for adaptive control system in tropical smart greenhouse

Folked Eduard Laumal<sup>1,3</sup>, Herry Suhardiyanto<sup>2</sup>, Mohamad Solahudin<sup>2</sup>, Slamet Widodo<sup>2</sup>

<sup>1</sup>Department of Mechanical and Biosystem Engineering, Graduate Study Program on Agricultural Engineering Science, IPB University, Bogor, Indonesia

<sup>2</sup>Department of Mechanical and Biosystem Engineering, IPB University, Bogor, Indonesia

<sup>3</sup>Department of Computer Engineering, Politeknik Negeri Kupang, Kupang, Indonesia

## Article Info

### Article history:

Received Sep 27, 2022

Revised Jan 20, 2023

Accepted Feb 4, 2023

### Keywords:

Adaptive control system

Error based method

Non-parametric test

Sensor

Smart greenhouse

## ABSTRACT

The uniform control in greenhouse with technology capabilities is seemingly still difficult to be obtained due to the accuracy uncertainty of the data in certain locations. Considering this case, it is highly necessary to choose the right location for the sensor installation. This study aimed to determine sensor placement locations to support precision control activities, using an arch-type smart greenhouse measuring 8×24 m<sup>2</sup> as the research location. Air temperature was calculated from 12 locations and analyzed for all possible combinations to designate the best sensor point according to the number of sensors. The analysis was conducted using the error-based method to ascertain the number and location of sensors that represent the smart greenhouse. The best location and number of sensors are identified with performance value under 10% and recommended for developing an adaptive control system.

This is an open access article under the [CC BY-SA](https://creativecommons.org/licenses/by-sa/4.0/) license.



## Corresponding Author:

Herry Suhardiyanto

Department Mechanical and Biosystem Engineering

Graduate Study Program on Agricultural Engineering Science, IPB University

Bogor, West Java, Indonesia

Email: herrysuhardiyanto@apps.ipb.ac.id

## 1. INTRODUCTION

In general, greenhouses are developed in two ways: the traditional model, which relies on the natural climate to support plant growth, and the modern model, which involves various automatic control technologies to support control activity [1]–[3], which use IoT monitoring mechanisms [4], [5] or wireless technology for communication [6]. Several control technology systems for greenhouses have been carried out by Wan *et al.* [7], who developed an ESP8266-based temperature and humidity controller and placed it in the middle of the greenhouse to environment monitoring and remote control. Ardiansah *et al.* [8] developed a sensor-based automatic sustainable environment monitoring in greenhouses. Although control can be performed by systems developed for small greenhouses, improper placement of sensors in large greenhouses affects the uniformity and accuracy of control. Non-uniform control can impact the growth of plants inside the greenhouse.

Several studies about the placement of sensors have been carried out by several researchers, including Ostachowicz *et al.* [9], Oleynik *et al.* [10], Yang *et al.* [11], Suryanarayana *et al.* [12], Chen and Gorle [13] and Jaya *et al.* [14]. These studies are an attempt to identify and determine the location of sensor placement for maximum control and productivity in cultivation. Hu *et al.* [15] succeeded in identifying sensor locations using a grey correlation degree method in a large-scale laying hen houses. This strategy not only meets the goal of accurately monitoring the hen house temperature, but also saves the hardware cost,

which has important application value. Guenther and Sawodny [16] succeeded in simulating the distribution of air temperature using Gaussian regression model and computational fluid dynamics (CFD) and recommending the location and number of sensors in a greenhouse. Lee *et al.* [17] measured the temperature and humidity in the chicken coop for 52 locations at a height of 0.3 m above the floor and calculated the temperature-humidity index (THI) using the Kriging method. Three locations with the lowest, middle, and highest THI were chosen as ideal sensor points because the cage's inner environment had mechanical ventilation. Lee *et al.* [18] also developed a mechanism for determining the optimal sensor location in a traditional greenhouse type and succeeded in recommending a sensor placement location that is representative of the traditional greenhouse.

Some of the studies above have recommended the location of sensor placement in the room but have not considered the structure of the room and the number of sensors that must be installed. Without using a quantitative approach, greenhouse developers still choose sensor locations by estimating locations with the smallest temperature changes. Despite the fact that the placement of sensors representing the internal environment has to be determined by data-driven quantitative studies. This research aims to determine the location and number of sensors that are representative of the smart greenhouse environment, to improve the performance of adaptive environmental control with technological devices. Air temperature was chosen as an environmental parameter because it is one of the important growth variables that can be measured simultaneously at multiple locations.

## 2. METHOD

This study was conducted at the Siswadi Soepardjo Field Laboratory, Department of Mechanical Engineering and Biosystems of IPB, in an arch-type tropical smart greenhouse in Figure 1, measuring  $8 \times 24$  m<sup>2</sup>, oriented south-north, with a roof of 2.5 m and a ridge of 7.5 m, as shown in Figure 1(a). The cultivation room measured  $\pm 150$  m<sup>2</sup> ( $7.5 \times 20$  m) with five rows of parallel planting shelves, as shown in Figure 1(b). Meanwhile, the control room is used to locate mechanical devices, such as the evaporative cooler, fogger, and nutrients. The building structure has an evaporative cooling system and a water chiller placed separately.

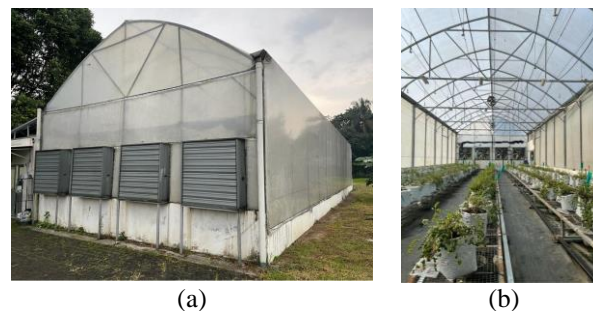


Figure 1. Tropical smart greenhouse: (a)  $8 \times 24$  m<sup>2</sup> arch smart greenhouse IPB and (b) internal environment

### 2.1. Data exploration

Figure 2 shows the layout of locations in the smart greenhouse as a reference for sensor placement. There are 12 locations grouped into three layers with a height of 0.65 m ( $h_1$ : 1, 4, 7, 10), 1.65 m ( $h_2$ : 2, 5, 8, 11), and 2.75 m ( $h_3$ : 3, 6, 9, 12). All locations are arranged vertically in the center of the room.

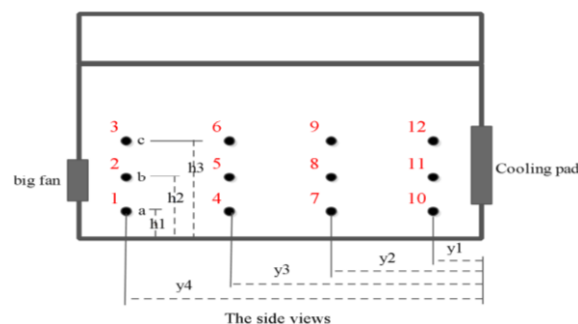


Figure 2. Schematic of measuring air temperature parameter in smart greenhouse

Air temperature data were collected at 12 locations using a thermocouple cable for four days from 06:00 to 18:00, then explored to determine the distribution and variability based on the maximum, minimum, average, and standard deviation. Non-parametric tests were used to determine the significance of data differences at each point. Furthermore, fulfillment of assumptions becomes the basis for identifying sensor locations using error-based methods, with root mean percentage error (RMSE) and mean absolute percentage error (MAPE) as performance indicators. The sensor location determination chart is shown in Figure 3.

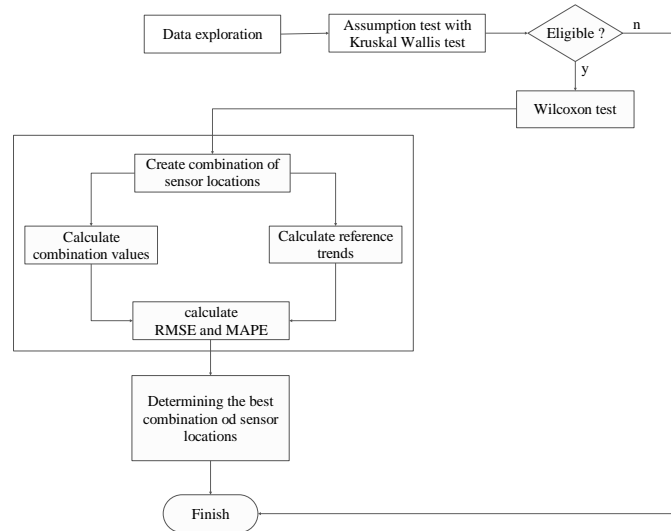


Figure 3. Data processing scheme for determining the optimal sensor location

**2.2. Non-parametric test**

Kruskal Wallis and Wilcoxon tests are non-parametric testing methods used to determine significant differences in data when there is a violation of assumptions in the ANOVA test [19], [20]. The assumptions should be achieved  $H_0$ : the temperature at the 12 sensor locations is the same, and  $H_1$ : the temperature is not the same. There is no significant difference between the  $i^{th}$  and the  $j^{th}$  sensor locations when  $H_0$  is met. Meanwhile, there is a significant difference between the sensor locations when  $H_1$  is met since verification is carried out using the Wilcoxon test with  $p < 0.05$ . The non-parametric test was constructed using RStudio 4.0.2 software.

**2.3. Error calculation**

An error calculations are performed to select a combination of sensor that represents the entire environment [18], [21]. Sensor combinations are calculated with the equation  $2^n - 1$  ( $n$ =number of location points), then the air temperature of each combination is compared with the average air temperature to calculate the performance index. The calculation of the performance index is done by parallel computation built through RStudio programming due to the large number of point combinations and shorter time. Furthermore, the MAPE and RMSE in (1) and (2) are used to calculate the accuracy of data from sensor locations [22]. MAPE provides information on how much the forecasting error is compared to the actual value [23]. The smaller the percentage error in MAPE, the more accurate the performance of the forecasting results. The variations of MAPE values are grouped into four performance scales as shown in Table 1, according to Lewis' concept, which was reused by Liu *et al.* [24] to study natural gas consumption using a new gray fractional model, and Vaugan *et al.* [25] who explored machine learning-based COVID-19 challenges. In this study, the combination of the smallest MAPE will be recommended as the sensor location.

$$MAPE = \frac{100}{n} \sum_{i=1}^n \left| \frac{R_i - C_i}{R_i} \right| \tag{1}$$

$$MAPE = \frac{100}{n} \sum_{i=1}^n \left| \frac{R_i - C_i}{R_i} \right| \tag{2}$$

RMSE expressed in °C, MAPE in %,  $n$ =total number of data,  $R_i$ =reference trend value at a given time, and  $C_i$ =combination trend value at a given time.

Table 1. Grouping of MAPE presentation values according to Lewis' concept

MAPE values	Performance
< 10%	Very good
10%-20%	Good
20%-50%	Good enough
> 50%	Poor

### 3. RESULTS AND DISCUSSION

#### 3.1. Environmental data exploration

Air temperature measurements at 12 location points inside the smart greenhouse for four days produced 7,236 data which were further explored. The distribution of each location against the external temperature, average room temperature, and solar energy intensity is presented in Figure 4. The average air temperature inside the smart greenhouses during the four days of measurement (T-reference) was lower than the external (T-out) due to the chiller's continuously delivering water to the cooling pad to minimize thermal stress. The cooling pad provides changes in air temperature and humidity [26] and affects the performance efficiency of the house system even with different materials [27], [28]. Despite the high solar energy intensity, the chiller activity reduced the air temperature inside the smart greenhouse. The air temperature inside the smart greenhouse reached its highest and lowest value at 32 °C and 24 °C, which is 2 °C and 1 °C lower than the outside, respectively.

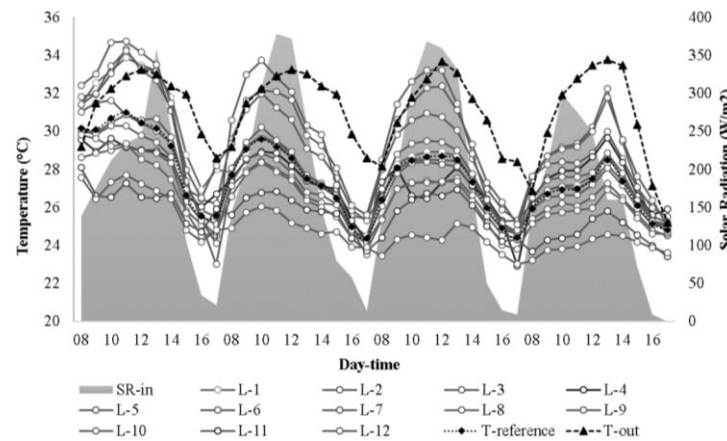


Figure 4. The air temperature was measured at 12 points inside and outside the smart greenhouses for four days

A summary of data at 12 location points with different heights inside the smart greenhouse is presented in Table 2. During the four days of measurement, the lowest average temperature occurred in point 4 at 22.8 °C, and the highest was point 9 at 33.7 °C. The largest standard deviations were points 1, 9, and 10, indicating high variability in the data. Three pairs of locations with similar temperature patterns were found at locations 1 and 9, 3 and 10, and 4 and 8, while the others differed.

Table 2. Summary of descriptive statistics of air temperature at 12 locations points in the smart greenhouse

Point location	Mean (°C)	STD	Min (°C)	Max (°C)	Range	Coefficient of variation	Q1	Q2	Q3
1	29.85	2.00	25.5	32.5	7.0	0.07	28.1	30.7	31.40
2	27.75	1.29	24.6	29.8	5.2	0.05	26.8	28.1	28.80
3	29.18	1.97	25.1	31.9	6.8	0.07	27.3	29.9	30.80
4	27.44	1.60	22.8	32	9.4	0.06	26.5	27.6	28.60
5	27.52	1.42	24.4	29.9	5.5	0.05	26.2	28.0	28.67
6	28.32	1.89	24.4	31.2	6.8	0.07	26.5	29.0	29.87
7	26.70	1.20	23.8	29.2	5.4	0.05	25.7	27.1	27.62
8	27.39	1.68	23.3	30	6.7	0.06	25.9	28.0	28.75
9	29.79	2.90	24.2	33.7	9.5	0.10	26.8	30.8	32.30
10	29.27	2.08	25.1	32.5	7.4	0.07	27.4	30.0	30.95
11	25.61	0.86	23.4	27.8	4.4	0.03	24.9	25.7	26.22
12	24.95	0.71	22.9	26.7	3.8	0.03	24.4	25.0	25.45

The distribution of air temperature data using the boxplot is given in Figure 5. The highest interquartile range is point 9, at a value of 9.5 and a standard deviation of 2.90. The lowest interquartile content is point 12 at 0.71 for the standard deviation value. Based on Table 2 and Figure 5, the pairs of locations with similar air temperature data distribution are 1 and 9 with mean values of 29.85 and 29.79, pairs 3 and 10 with mean values of 29.18 and 29.27, pairs 4 and 8 with mean values of 27.44 and 27.39. Apart from these pairs, the air temperature data are spread differently.

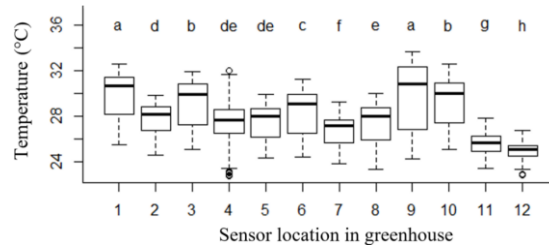


Figure 5. Boxplot of air temperature distribution at 12 points location inside the smart greenhouse

### 3.2. Non-parametric test

This study used Kruskal Wallis and Wilcoxon to test the uniformity of data at each sensor location. The results with a reference value of 0.05 obtained a p-value of  $2.2e-16$ , or smaller than the reference value, hence,  $H_0$  is rejected, and the air temperature is not uniform. Furthermore, the Wilcoxon test with a reference value of 0.05 found that pairs 1 and 9, 4 and 5, and 4 and 8 had p-values  $>0.05$ , namely 0.46, 0.18, and 0.53, respectively. This indicated there is no significant difference in the three pairs of locations, while for the others, there is a significant difference at p-value  $<0.05$ . The results of the data exploration and homogeneity test showed that there were significant differences in the data at 12 location points. Therefore, an error-based method was necessary to select the optimal sensor location.

### 3.3. Sensor location determination

The sensor location was determined by analyzing the difference in air temperature at 12 locations in the smart greenhouse against the average, as shown in Figure 6. The thin line shows the air temperature at each location point, while the bold indicates the reference. Furthermore, the reference is the average temperature of all site points and represents the value inside the smart greenhouse.

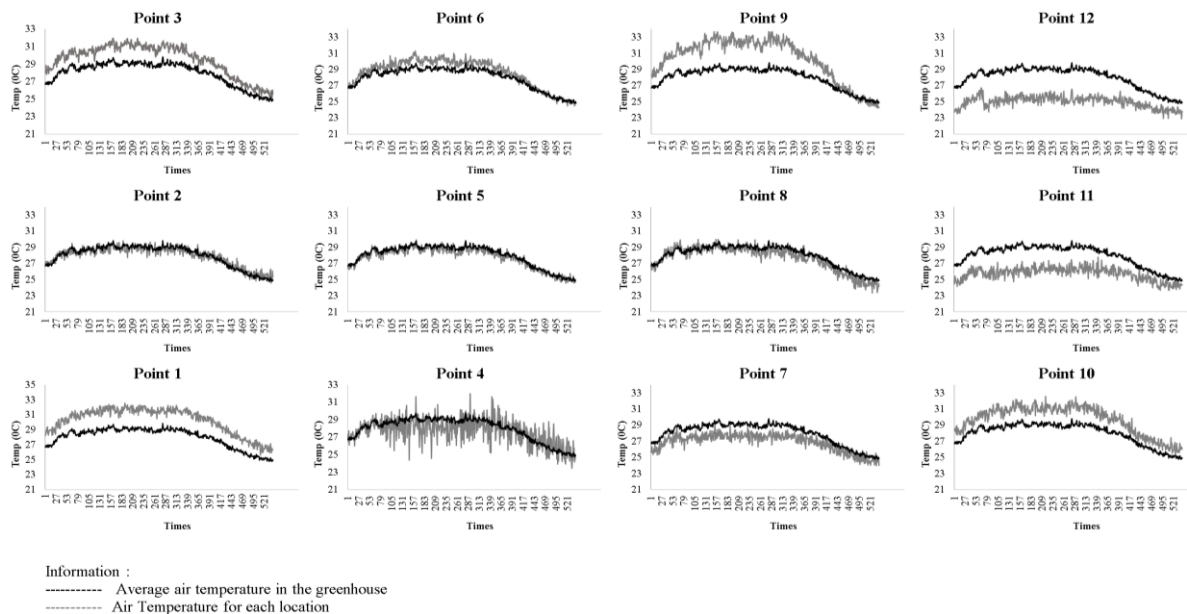


Figure 6. Comparison of air temperature at each measurement point location with the average smart greenhouse temperature for four days from 06.00 to 18.00

In each layer, the air temperature trend appears to decrease towards the cooling pad. Different conditions occur at points 9 and 10 with air temperatures higher than the reference due to unavoidable extreme data. Sensor location with trends similar to the reference air temperature is seen at points 2, 5, and 8. Meanwhile, sensor location with higher air temperatures value is seen at points 1, 3, 6, 9, and 10, while those with low air temperatures are seen at 4, 7, 11, and 12. The point recommended as the sensor location is the air temperature trend closest to the average. The similarity of the pattern influences the likeliness of being selected as a sensor location [29]. The 12 points inside the smart greenhouse have different air temperature distributions, but points 2, 4, 5 and 8 are most likely recommended for sensor locations.

The combination of the 12 sensor locations with the 2<sup>n</sup>-1 equality obtained 4095. The air temperature from each combination is compared with the reference air temperature using RMSE and MAPE to obtain the smallest error. Figures 7 to 10 show some results of sensor location programming based on RMSE and MAPE values, for 1 to 4 sensor combinations.

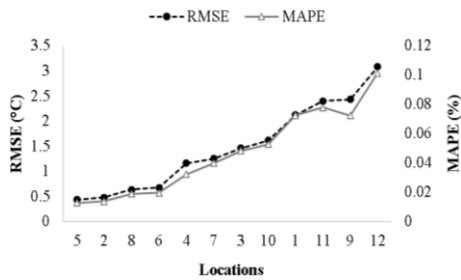


Figure 7. Combination of 1 sensor location in order of MAPE and RMSE values

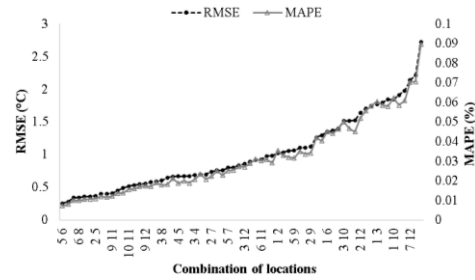


Figure 8. Combination of 2 sensor locations in order of MAPE and RMSE values

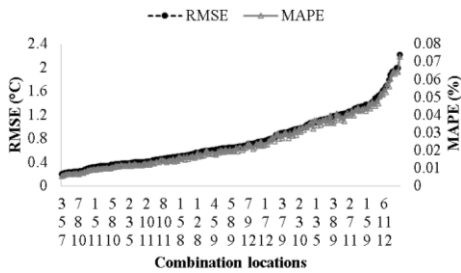


Figure 9. Combination of 3 sensor locations in order of MAPE and RMSE values

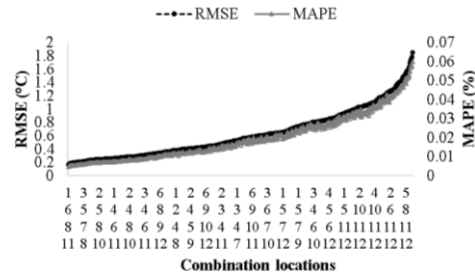


Figure 10. Combination of 4 sensor locations in order of MAPE and RMSE values

The combination of one sensor location, as shown in Figure 7, point 5 has the smallest RMSE and MAPE values of 0.43 °C and 1.26%, followed by point 2 with values of 0.48 °C and 1.38%, point 8 with values of 0.83 °C and 1.89%. The combination of 2 locations, as shown in Figure 8, has 66 possibilities, with the lowest RMSE and MAPE values obtained in 5-6, which are 0.25 °C and 0.07%. The following combinations are 3-7 and 2-6, with RMSE and MAPE values of 0.28 °C, 0.8 %, and 0.34 °C, 0.1%, respectively. Meanwhile, the combination with the highest values is 11-12 with values of 2.72 °C and 0.89%. Points 5 and 6 are at altitudes of 1.75 m and 2.75 m but are in the second and third layers, y3 away from the cooling pad.

The combination of 3 locations, as shown in Figure 9, has 220 possibilities, with the lowest RMSE and MAPE values being in the 3-5-7 of 0.19 °C and 0.06%. The next combinations are 2-5-6 and 3-10-12 with values of 0.21 °C, 0.06%, and 0.22 °C, 0.06%, respectively. Vertically, points 3, 5, and 7 are at an altitude of 2.75 m, 1.75 m, and 0.65 m, y4, y3, and y2 away from the cooling pad, respectively. The 4 locations in Figure 10 have 495 possibilities with the lowest RMSE and MAPE values in the combination of 1-6-8-11 with 0.17 °C and 0.05%. Combinations 1-5-6-11 and 1-3-8-12 are second and third with RMSE and MAPE values of 0.176 °C, 0.05% and 0.18 °C, 0.053%, respectively.

**3.4. Evaluation of the best location and number of sensors**

The sensor location combinations are inversely related to RMSE and MAPE. The more combinations, the lower the RMSE and MAPE values, the more similar the air temperature values are

compared to the average air temperature. Figure 11 shows the comparison the air temperature at 12 points and the average room air temperature based on the number of sensors. Figure 11(a) displays the RMSE value, and Figure 11(b) displays the MAPE value, both of which are generated by the error-based method.

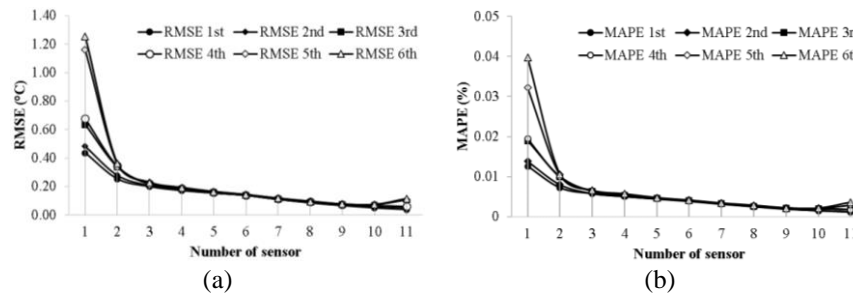


Figure 11. Error trend of 6 sensor location combinations with error-based method: (a) RMSE value and (b) MAPE value

The decrease in error value is quite significant when there is a change from 1 to 2 sensors, with a difference of 0.18 °C and 0.54% for RMSE and MAPE. However, this decrease has no effect because the MAPE value for one sensor location is lower than 10% or has excellent performance. Even though the sensors represent the internal environment of the greenhouse, the number affects the cost of providing devices when building an adaptive control system. Based on these conditions, this study recommends one sensor at point 5 as the best sensor location when developing an adaptive control system in an 8×12 m<sup>2</sup> arch-type greenhouse. The air temperature conditions measured at that point are considered representative of the entire internal environment.

### 3.5. Validation of the best sensor location

The RMSE and MAPE were validated using air temperature data recorded at point 5 for 2 days and compared with the reference air temperature as shown in Figure 12. The air temperature movement on the first day fluctuated slightly in the morning and afternoon, while on the second day the movement was more similar to the reference air temperature. The results of the RMSE and MAPE calculations were obtained as 0.02 °C and 1.6%, still under 10%. Therefore, the performance of 1 sensor at point 5 is said to be very good and is recommended for use in adaptive control systems that use an internal air temperature parameter as part of the control decision-making process.

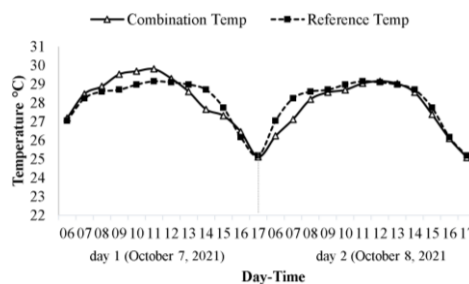


Figure 12. Comparison of the air temperature value at point 5 with the average air temperature of the smart greenhouse during two days of measurement using the sensor

## 4. CONCLUSION

Kruskal-Wallis’s test results have shown significant data differences at 12 locations in the smart greenhouse. The Wilcoxon test found pairs of sensor locations that were not significantly different: points 1-9, 4-5, and 4-8. Other locations that are significantly different require further study to determine sensor locations that represent the smart greenhouse environment. The error-based methods with different heights obtained the best sensor location at point 5 with RMSE and MAPE of 0.43 °C and 1.26%, respectively. The validation for two days resulted in RMSE and MAPE values of 0.02 °C and 1.6%, respectively, so the air

temperature at point 5 can represent the overall air temperature inside the  $8 \times 12 \text{ m}^2$  arch-type smart greenhouse. When an adaptive control system is developed for this smart greenhouse, and using the internal air temperature parameter, the placement of sensor at point 5 will provide better performance, as the air temperature data processed for control decisions, truly describes the air temperature conditions inside the smart greenhouse.

## ACKNOWLEDGEMENTS

The authors would like to thank the Indonesia Endowment Funds for Education (LPDP), a non-echelon work unit at the Ministry of Finance, for funding this research.

## REFERENCES




- [1] A. Badji, A. Benseddik, H. Bensaha, A. Boukhelifa, and I. Hasrane, "Design, technology, and management of greenhouse: A review," *Journal of Cleaner Production*, vol. 373, p. 133753, Nov. 2022, doi: 10.1016/j.jclepro.2022.133753.
- [2] A. Ajagekar and F. You, "Deep reinforcement learning based automatic control in semi-closed greenhouse systems," *IFAC-PapersOnLine*, vol. 55, no. 7, pp. 406–411, 2022, doi: 10.1016/j.ifacol.2022.07.477.
- [3] Y. Wu *et al.*, "Remote-control system for greenhouse based on open source hardware," *IFAC-PapersOnLine*, vol. 52, no. 30, pp. 178–183, 2019, doi: 10.1016/j.ifacol.2019.12.518.
- [4] A. Kochhar and N. Kumar, "Wireless sensor networks for greenhouses: An end-to-end review," *Computers and Electronics in Agriculture*, vol. 163, p. 104877, Aug. 2019, doi: 10.1016/j.compag.2019.104877.
- [5] J. Wang, M. Chen, J. Zhou, and P. Li, "Data communication mechanism for greenhouse environment monitoring and control: An agent-based IoT system," *Information Processing in Agriculture*, vol. 7, no. 3, pp. 444–455, Sep. 2020, doi: 10.1016/j.inpa.2019.11.002.
- [6] J. Feng and X. Hu, "An IoT-based hierarchical control method for greenhouse seedling production," *Procedia Computer Science*, vol. 192, pp. 1954–1963, 2021, doi: 10.1016/j.procs.2021.08.201.
- [7] Z. Wan, Y. Song, and Z. Cao, "Environment dynamic monitoring and remote control of greenhouse with ESP8266 NodeMCU," in *Proceedings of 2019 IEEE 3rd Information Technology, Networking, Electronic and Automation Control Conference, ITNEC 2019*, Mar. 2019, pp. 377–382, doi: 10.1109/ITNEC.2019.8729519.
- [8] I. Ardiansah, N. Bafdal, E. Suryadi, and A. Bono, "Design of micro-climate data monitoring system for tropical greenhouse based on arduino UNO and raspberry pi," *IOP Conference Series: Earth and Environmental Science*, vol. 757, no. 1, p. 012017, May 2021, doi: 10.1088/1755-1315/757/1/012017.
- [9] W. Ostachowicz, R. Soman, and P. Malinowski, "Optimization of sensor placement for structural health monitoring: a review," *Structural Health Monitoring*, vol. 18, no. 3, pp. 963–988, May 2019, doi: 10.1177/1475921719825601.
- [10] A. Oleynik, M. I. G. Ibáñez, N. Blaser, A. Omar, and G. Alendal, "Optimal sensors placement for detecting CO<sub>2</sub> discharges from unknown locations on the seafloor," *International Journal of Greenhouse Gas Control*, vol. 95, p. 102951, Apr. 2020, doi: 10.1016/j.ijggc.2019.102951.
- [11] C. Yang, K. Liang, X. Zhang, and X. Geng, "Sensor placement algorithm for structural health monitoring with redundancy elimination model based on sub-clustering strategy," *Mechanical Systems and Signal Processing*, vol. 124, pp. 369–387, Jun. 2019, doi: 10.1016/j.ymsp.2019.01.057.
- [12] G. Suryanarayana, J. Arroyo, L. Helsen, and J. Lago, "A data driven method for optimal sensor placement in multi-zone buildings," *Energy and Buildings*, vol. 243, p. 110956, Jul. 2021, doi: 10.1016/j.enbuild.2021.110956.
- [13] C. Chen and C. Gorié, "Optimal temperature sensor placement in buildings with buoyancy-driven natural ventilation using computational fluid dynamics and uncertainty quantification," *Building and Environment*, vol. 207, p. 108496, Jan. 2022, doi: 10.1016/j.buildenv.2021.108496.
- [14] M. M. Jaya, R. Ceravolo, L. Z. Fragonara, and E. Matta, "An optimal sensor placement strategy for reliable expansion of mode shapes under measurement noise and modelling error," *Journal of Sound and Vibration*, vol. 487, p. 115511, Nov. 2020, doi: 10.1016/j.jsv.2020.115511.
- [15] X. Hu, L. Gao, L. Huo, L. Li, and M. Er, "Optimal placement of laying Hen house temperature sensors based on genetic algorithm," *IEEE Access*, vol. 10, pp. 7234–7244, 2022, doi: 10.1109/ACCESS.2022.3141090.
- [16] J. Guenther and O. Sawodny, "Optimal sensor placement based on gaussian process regression for shared office spaces under various ventilation conditions," in *Conference Proceedings - IEEE International Conference on Systems, Man and Cybernetics*, Oct. 2019, vol. 2019-Octob, pp. 2883–2888, doi: 10.1109/SMC.2019.8914297.
- [17] S. Lee, G. Park, and I. B. Lee, "Optimal sensor placement for temperature monitoring inside broiler houses," in *10th International Livestock Environment Symposium (ILES X)*, 2018, doi: 10.13031/iles.18-121.
- [18] S. Lee, I. Lee, U. Yeo, R. Kim, and J. Kim, "Optimal sensor placement for monitoring and controlling greenhouse internal environments," *Biosystems Engineering*, vol. 188, pp. 190–206, 2019, doi: https://doi.org/10.1016/j.biosystemseng.2019.10.005.
- [19] J. T. E. Richardson, "Kruskal-Wallis Test," in *The SAGE Encyclopedia of Educational Research, Measurement, and Evaluation*, B. B. Frey, Ed. SAGE Publications, 2018, pp. 937–939.
- [20] J. S. C. Clark, P. Kulig, K. Podsiadło, and K. Rydzewska, "Kruskal-Wallis Power Studies Utilizing Bernstein Distributions; preliminary empirical studies using simulations / medical studies." 2020, arXiv: 2110.11676.
- [21] G. Krishna and A. K. Saha, "Optimal sensor spacing in IoT network based on quantum computing technology," *International Journal of Parallel, Emergent and Distributed Systems*, vol. 38, no. 1, pp. 58–84, Jan. 2023, doi: 10.1080/17445760.2022.2126975.
- [22] N. K. Rai, D. Saravanan, L. Kumar, P. Shukla, and R. N. Shaw, "RMSE and MAPE analysis for short-term solar irradiance, solar energy, and load forecasting using a recurrent artificial neural Network," in *Applications of AI and IOT in Renewable Energy*, 2022, pp. 181–192.
- [23] D. Chicco, M. J. Warrens, and G. Jurman, "The coefficient of determination R-squared is more informative than SMAPE, MAE, MAPE, MSE and RMSE in regression analysis evaluation," *PeerJ Computer Science*, vol. 7, pp. 1–24, Jul. 2021, doi: 10.7717/PEERJ-CS.623.






- [24] C. Liu, W. Z. Wu, W. Xie, T. Zhang, and J. Zhang, "Forecasting natural gas consumption of China by using a novel fractional grey model with time power term," *Energy Reports*, vol. 7, pp. 788–797, Nov. 2021, doi: 10.1016/j.egy.2021.01.082.
- [25] L. Vaughan *et al.*, "An exploration of challenges associated with machine learning for time series forecasting of COVID-19 community spread using wastewater-based epidemiological data," *Science of the Total Environment*, vol. 858, p. 159748, Feb. 2023, doi: 10.1016/j.scitotenv.2022.159748.
- [26] S. Kumar, S. S. Salins, S. V. K. Reddy, and P. S. Nair, "Comparative performance analysis of a static & dynamic evaporative cooling pads for varied climatic conditions," *Energy*, vol. 233, p. 121136, Oct. 2021, doi: 10.1016/j.energy.2021.121136.
- [27] D. Misra and S. Ghosh, "Evaporative cooling technologies for greenhouses: A comprehensive review," *Agricultural Engineering International: CIGR Journal*, vol. 20, no. 1, pp. 1–15, 2018.
- [28] A. Hegazy, M. Farid, A. Subiantoro, and S. Norris, "Sustainable cooling strategies to minimize water consumption in a greenhouse in a hot arid region," *Agricultural Water Management*, vol. 274, p. 107960, Dec. 2022, doi: 10.1016/j.agwat.2022.107960.
- [29] E. Levintal *et al.*, "eGreenhouse: Robotically positioned, low-cost, open-source CO2 analyzer and sensor device for greenhouse applications," *HardwareX*, vol. 9, p. e00193, Apr. 2021, doi: 10.1016/j.ohx.2021.e00193.

## BIOGRAPHIES OF AUTHORS






**Folkes Eduard Laumal**    is a doctoral student in the agricultural engineering science study program, department of mechanical and biosystem engineering, IPB. He entered IPB in 2019 and is currently completing research with the title "design of adaptive control systems for smart greenhouse in hot and humid climates" under the promoter team of Prof. Dr. Ir. Herry Suhardiyanto, M.Sc., Dr. Ir. Mohamad Solahudin, M.Sc., and Dr. Slamet Widodo, STP., M.Sc. Of the five sub-topics of the dissertation being carried out, this paper is the one that has been completed. The conclusion of this paper is used as a recommendation for placing adaptive control devices, where the location and number of sensors are adjusted to the conclusions of this paper. It is expected that the control system can work optimally. He can be contacted via email address: folkeslaumal76@gmail.com.






**Herry Suhardiyanto**    completed his doctoral program in agricultural engineering at Ehime University, Japan, in 1994, as a professor in agricultural technology at the department of mechanical and biosystem engineering, faculty of agricultural technology, IPB. As Chancellor of IPB for the period 2007–2017. Several kinds of research on heat transfer, cooling systems, and neural network modelling have been published in national and international scientific journals. Heat transfer in aeroponic chambers with zone cooling applications in the biophysics journal, heat transfer analysis on the main pipe of hydroponic systems with nutrient solution cooling and heat transfer analysis on cooling pipes for root zone cooling systems, in the *Jurnal Keteknik Pertanian*. He can be contacted at email: herrysuhardiyanto@apps.ipb.ac.id.



**Mohamad Solahudin**    completed the doctoral program in agricultural engineering at the agricultural engineering study program, faculty of agricultural technology, IPB, in 2013 with a dissertation titled the development of weed control methods in computational multi-agent-based precision agriculture. He pursues the field of expert systems and computing, with several studies published in national and international journals. Some of them are: Weed detection using fractal-based low-cost commodity hardware raspberry Pi, in the *Indonesian Journal of Electrical Engineering and Computer Science*, assessment of pre-treatment and classification methods for Java paddy field cropping pattern detection on MODIS images on *Remote Sensing Applications Journal: Society and Environment*. He can be contacted at email: msoul9@yahoo.com.



**Slamet Widodo**    completed his doctoral program at Kyoto University, Japan, in 2013 with the dissertation titled wind and doppler shift compensation for spread spectrum sound-based positioning system. A lot of research in instrumentation field and automatic control with several publications in national and international journals. Control system for nutrient solution of nutrient film technique using fuzzy logic, in *Telkomnika Journal*, modification of NIR instruments for fast and non-destructive determination of chemical content of organic materials, in *Agricultural Engineering Journal*, combined fluorescence-transmittance imaging system for geographical authentication of patchouli oil, in *Spectrochimica Acta (SSA) Journal*, application of microwave energy for warehouse pest control *araecerus fasciculatus* on cocoa beans in *Agricultural Engineering Journal*. He can be contacted at email: slamet\_ae39@apps.ipb.ac.id.